Effects of relative phase and interactions on atom-laser outcoupling from a double-well Bose-Einstein condensate: Markovian and non-Markovian dynamics

G. M. Nikolopoulos[1], C. Lazarou[2] and P. Lambropoulos[1,3]

[1] Institute of Electronic Structure and Laser, FORTH, P. O. Box 1527, Heraklion 711 10, Crete, Greece
[2] Department of Physics and Astronomy, University of Sussex, Brighton BN1 9QH, United Kingdom
[3] Department of Physics, University of Crete, P. O. Box 2208, Heraklion 71003, Crete, Greece

Abstract. We investigate aspects of the dynamics of a continuous atom-laser scheme based on the merging of independently formed atomic condensates. Our theoretical analysis covers the Markovian as well as the non-Markovian operational regimes, and is based on a semiclassical (mean-field) two-mode model. The role of the relative phase between the two condensates and the effect of interatomic interactions on the evolution of the trapped populations and the distribution of outcoupled atoms are discussed.

PACS numbers: 03.65.Yz,03.75.Pp

1. Introduction

The dynamics of the atom laser, beyond the Born and Markov approximations have been investigated mostly in the framework of a rather simple model, involving a single condensate mode coherently coupled to a continuum of free-space modes [1, 2, 3, 4, 5, 6]. In recent work [7], we extended this model to a two-mode scenario. Specifically, we considered two initially independent Bose-Einstein condensates (BECs) consisting of a large number of bosonic atoms cooled into the lowest eigenmode of their respective traps. The two traps are assumed brought together, while atoms are outcoupled coherently from one of the traps only, whose condensate mode plays the role of the "lasing mode" which is replenished with atoms from the other trap, which serves as a "pump". The chief motivation for this investigation came from the experiment of Chikkatur et al. [8] on the merging of BECs, which offers a conceptually simple scenario for a continuous atom laser. The main idea in that work relies on replenishing the condensate mode of the lasing trap by transfering other independently formed BECs using optical tweezers.

The theoretical modelling of such a scenario has to cope with a reasonable description of the condensates, the non-Markovian character of the coupling to the atomic continuum, as well as the interatomic interactions present in the system. In an attempt to understand how the presence of the second condensate affects the atom-laser dynamics, we focused first on an interaction-free model, assuming in addition a vanishing relative phase between the two condensates [7]. Even within these two simplifications, the system was found to exhibit a number of interesting features such as the formation of a bound state in the strong-outcoupling regime, as well as a dark line in the spectrum of the outcoupled atoms. In the present paper, we relax both of the above simplifying assumptions, addressing thus a more realistic scenario which takes into account inter-particle interactions and a non-vanishing relative phase between the two independent BECs. As one might have anticipated, a number of new features emerge in the time-development of the system as well as the spectrum of the outcoupled atoms.

In brief, the interplay among several parameters such as the changing chemical potentials due to the outcoupling, the strength of the interparticle interactions (nonlinearity), as well as the strength of the outcoupling, set the stage for the appearance of a Josephson effect which competes with self-trapping, and also chirping, i.e. a variation of the energies of the outcoupled atoms.

2. The system

Our system consists of two independently prepared, elongated BECs (A and B), with N being the total number of atoms in the system. The two traps are initially far apart and each BEC experiences only its local potential, while only the lowest level of each trap (condensate mode) is populated. To allow for the merging of the two BECs, trap B is moved towards trap A along the radial direction x, while at the same time atoms are outcoupled coherently from BEC A, by applying external electromagnetic fields (see Ref. [7] for a detailed description of the system under consideration). Hence, to point out the discrete roles of the two BECs, from now on we also refer to BEC A as the "lasing condensate" and to BEC B as the "pumping condensate".

Presently, transport of BECs can be realized efficiently using optical tweezers which are produced by focused laser beams and offer limited trap volume and depth

[8]. Hence, during the merging process the two BECs can be brought as close as the traps' beam waist, before they start affecting each other. To be consistent with the experimental setup for BEC merging [8] as well as related theoretical work [9, 10], we assume two nearly identical axially symmetric harmonic traps with confining frequencies ω_z and $\omega_x = \omega_y = \omega_\perp$. The atomic density profiles adiabatically follow the movement of the traps, while the global potential experienced by the trapped atoms can be modeled by a time-dependent double-well potential [7]. In general, besides the merging time-scale $t_{\rm m}$, the details of the motion of trap B are not of great importance [8, 9, 10]. The crucial point is that the BEC merging must be adiabatic so that any kind of excitations in the system are suppressed.

The outcoupling mechanism under consideration is based on the application of external electromagnetic fields which induce an atomic transition from the internal state ($|t\rangle$) of the trapped atoms to an untrapped state $|f\rangle$. The outcoupled atoms are guided through an atomic waveguide [11, 12], thus resulting in an effective one-dimensional atom laser propagating along the weak confining axis of the waveguide. Such a guided atom laser has been demonstrated recently by Guerin *et al.* [13] and offers many advantages over the conventional outcoupling schemes. Formally speaking, the strong transverse confinement allows us to assume that the transverse dynamics of the free atoms adiabatically follow the slowly varying transverse potential of the optical guide [13], which is assumed to be nearly the same with the transverse potential of trap A. In the absence of gravitational or other forces (as in the experimental setup [13]), the longitudinal component of the potential is practically zero and the outcoupled atoms propagate freely along the z direction.

2.1. Two-mode model

During the merging, the condensate wavefunctions start overlapping in space as the two traps approach each other along the x direction, and a Josephson-type tunneling is established between the two BECs. If the position uncertainty in the ground state of the traps is much smaller than the separation of the minima of the global potential, the overlap (and thus the Josephson coupling J) is small enough so that only the ground states of the traps are relevant. In first-order perturbation theory, the corresponding local ground-state wavefunctions $\varphi_{\rm A(B)}(\mathbf{r})$ are orthogonal and describe faithfully BEC A and B, at any time $0 < t \ll t_{\rm m}$ [14]. If in addition the effect of interatomic interactions on the ground-state properties of the two wells is small i.e., if

$$(\omega_x\omega_y\omega_z)^{1/3} \gg N\kappa, \tag{1}$$

where $\hbar\kappa$ is the onsite interaction energy per particle, the system under consideration is well-described in the framework of the standard two-mode model [14]. Introducing the sets of bosonic operators $\{\hat{a}^\dagger, \hat{a}\}$ and $\{\hat{b}^\dagger, \hat{b}\}$ for the description of the condensate modes A (lasing) and B (pumping), respectively, the Hamiltonian of the system reads [7]

$$\hat{\mathcal{H}} = \frac{\hbar\omega_z}{2}(\hat{a}^\dagger\hat{a} + \hat{b}^\dagger\hat{b}) + \hbar\sum_k \omega_k \hat{c}_k^\dagger\hat{c}_k + \hbar\kappa(\hat{a}^\dagger\hat{a}^\dagger\hat{a}\hat{a} + \hat{b}^\dagger\hat{b}^\dagger\hat{b}\hat{b}) + \hbar J(\hat{a}^\dagger\hat{b} + \hat{b}^\dagger\hat{a})$$
$$+\hbar\sum_k g(k,t)(\hat{a}\hat{c}_k^\dagger + \hat{a}^\dagger\hat{c}_k) + \hbar e^{-\eta^2}\sum_k g(k,t)(\hat{b}\hat{c}_k^\dagger + \hat{b}^\dagger\hat{c}_k), \tag{2}$$

where $\hat{c}_k^\dagger(\hat{c}_k)$ is the creation(annihilation) bosonic operator of a free atom with momentum k, and frequency

$$\omega_k = \frac{\hbar k^2}{2m}, \tag{3}$$

with m the atomic mass. In deriving Hamiltonian (2) we have applied the rotating-wave approximation for the outcoupling Hamiltonian, while we have neglected higher-order cross-interaction terms. Moreover, it is worth noting here that although the outcoupling mechanism is applied to the lasing BEC only, atoms are also outcoupled from the pumping condensate; albeit with a much slower rate [compare the last two terms of Hamiltonian (2)]. This is due to the overlap of the two BEC wavefunctions and, as we will see later on, it may affect considerably the spectrum of the atom laser.

For a weakly-interacting bosonic gas satisfying (1), the ground-state wavefunctions are well approximated by Gaussians and thus analytic expressions for all the parameters entering the Hamiltonian are readily obtained [7]

$$J(t) = \omega_z \left(\frac{1}{2} + \frac{1}{\lambda} - \frac{\eta}{\lambda\sqrt{\pi}} \right) e^{-\eta^2}, \tag{4}$$

$$\kappa = \frac{\hbar a_{tt}}{\lambda m \sqrt{2\pi} l_z^3}, \tag{5}$$

$$g(k,t) = \frac{\sqrt{l_z}}{\pi^{1/4}} \sqrt{\Lambda(t)} e^{-k^2 l_z^2/2}, \tag{6}$$

where $\Lambda(t)$ is the coupling between trapped and untrapped atomic states, η is the dimensionless separation of the traps, $\lambda = \omega_z/\omega_x$, and $l_z \equiv \sqrt{\hbar/m\omega_z}$. In view of these relations, condition (1) yields the following upper bound on the total number of atoms we may consider in our simulations

$$N \ll \lambda^{1/3} \sqrt{2\pi} \frac{l_z}{a_{\rm tt}}, \tag{7}$$

where $a_{\rm tt}$ is the s-wave scattering length for collisions between trapped atoms.

2.2. The atomic continuum

The quadratic dependence of ω_k on k is responsible for a number of mathematical difficulties arising in the context of atom lasers [1]. For the one-dimensional atom-laser model under consideration, the density of states which are available to a free atom diverges at frequencies close to $\omega_{\rm e} = 0$, and is of the form

$$\rho(\omega) = \sqrt{\frac{m}{2\hbar\omega}} \Theta(\omega), \tag{8}$$

where $\Theta(\omega)$ is the usual step function. Taking advantage of the symmetrical shape of the coupling and the even parity of ω_k, the spectral response of the continuum for the particular outcoupling mechanism under consideration reads

$$D(\omega) \equiv 2|g(\omega,t)|^2 \rho(\omega) = \frac{\sqrt{2}\Lambda(t)}{\sqrt{\pi\omega_z}} \frac{e^{-2\omega/\omega_z}}{\sqrt{\omega}} \Theta(\omega), \tag{9}$$

where $g(\omega,t)$ is readily obtained from $g(k,t)$ using the atomic dispersion relation (3).

Clearly, the spectral response (9) does not vary slowly for all the frequencies and thus we are dealing with a structured continuum which, in general, invalidates both Born and Markov approximations. To address fundamental mathematical difficulties

associated with a continuum of this type, a number of new theoretical techniques have been developed [4, 15, 16, 17] over the last years. In the following, we adopt a discretization approach first developed in the context of photonic band-gap continua [18]. In the case of atom-lasers, the same technique has been shown capable of providing not only the evolution of the number of atoms in the condensates, but also the distribution of the outcoupled atoms in frequency domain, irrespective of the strength of the outcoupling and the form of the spectral response [6].

3. Heisenberg equations of motion

Given the Hamiltonian (2) one may proceed to derive Heisenberg equations of motion for the operators pertaining to the two traps and the continuum:

$$\frac{\mathrm{d}\langle\hat{a}\rangle}{\mathrm{d}t} = -\mathrm{i}\frac{\omega_z}{2}\langle\hat{a}\rangle - 2\mathrm{i}\kappa\langle\hat{a}^\dagger\hat{a}\hat{a}\rangle - \mathrm{i}J\langle\hat{b}\rangle - 2\mathrm{i}\int_0^\infty \mathrm{d}k g(k,t)\langle\hat{c}_k\rangle, \tag{10a}$$

$$\frac{\mathrm{d}\langle\hat{b}\rangle}{\mathrm{d}t} = -\mathrm{i}\frac{\omega_z}{2}\langle\hat{b}\rangle - 2\mathrm{i}\kappa\langle\hat{b}^\dagger\hat{b}\hat{b}\rangle - \mathrm{i}J\langle\hat{a}\rangle - 2\mathrm{i}e^{-\eta^2}\int_0^\infty \mathrm{d}k g(k,t)\langle\hat{c}_k\rangle, \tag{10b}$$

$$\frac{\mathrm{d}\langle\hat{c}_k\rangle}{\mathrm{d}t} = -\mathrm{i}\omega_k\langle\hat{c}_k\rangle - \mathrm{i}g(k,t)\langle\hat{a}\rangle - \mathrm{i}g(k,t)e^{-\eta^2}\langle\hat{b}\rangle. \tag{10c}$$

Due to the presence of interatomic collisions we have the appearance of third-order correlation functions on the right-hand side of equations (10a)-(10c). Thus, this set of equations is not closed, while consideration of differential equations for the third-order correlation functions leads to the appearance of terms of even higher order and so on. In general, there are no exact remedies for such mathematical problems, but an approximate solution can be always obtained by decorrelating higher-order correlation functions into products of lower ones.

In the present work we decorrelate the third-order correlation functions appearing on the right-hand side of equations (10a)-(10c) as follows: $\langle\hat{a}^\dagger\hat{a}\hat{a}\rangle \approx \langle\hat{a}^\dagger\rangle\langle\hat{a}\rangle\langle\hat{a}\rangle$ and $\langle\hat{b}^\dagger\hat{b}\hat{b}\rangle \approx \langle\hat{b}^\dagger\rangle\langle\hat{b}\rangle\langle\hat{b}\rangle$. We thus obtain the following closed set of coupled nonlinear differential equations

$$\frac{\mathrm{d}\langle\hat{a}\rangle}{\mathrm{d}t} = -\mathrm{i}\left(\frac{\omega_z}{2} + 2\kappa|\langle\hat{a}\rangle|^2\right)\langle\hat{a}\rangle - \mathrm{i}J\langle\hat{b}\rangle - 2\mathrm{i}\int_0^\infty \mathrm{d}k g(k,t)\langle\hat{c}_k\rangle, \tag{11a}$$

$$\frac{\mathrm{d}\langle\hat{b}\rangle}{\mathrm{d}t} = -\mathrm{i}\left(\frac{\omega_z}{2} + 2\kappa|\langle\hat{b}\rangle|^2\right)\langle\hat{b}\rangle - \mathrm{i}J\langle\hat{a}\rangle - 2\mathrm{i}e^{-\eta^2}\int_0^\infty \mathrm{d}k g(k,t)\langle\hat{c}_k\rangle, \tag{11b}$$

$$\frac{\mathrm{d}\langle\hat{c}_k\rangle}{\mathrm{d}t} = -\mathrm{i}\omega_k\langle\hat{c}_k\rangle - \mathrm{i}g(k,t)\langle\hat{a}\rangle - \mathrm{i}g(k,t)e^{-\eta^2}\langle\hat{b}\rangle. \tag{11c}$$

Although such a decorrelation is, in general, a crude approximation, it turns out to be equivalent to a higher-order decorrelation (mean-field approximation) of the form $\langle\hat{a}^\dagger\hat{a}\hat{a}\rangle \approx \langle\hat{a}^\dagger\hat{a}\rangle\langle\hat{a}\rangle$ and $\langle\hat{b}^\dagger\hat{b}\hat{b}\rangle \approx \langle\hat{b}^\dagger\hat{b}\rangle\langle\hat{b}\rangle$, when the two BECs are initially considered to be in coherent states.

It is worth noting here that, in the context of the semiclassical (mean-field) theory, the initial coherence of the condensate(s) is preserved in time. On the contrary, quantum models which go beyond the mean-field approximation predict a collapse of the condensate wavefunction (e.g., see [14, 19]). The time of collapse $t_\mathrm{c} \approx 1/(2\sqrt{N}\kappa)$ increases as we increase N with fixed κN, and thus the validity of the mean-field theory also improves. In any case, it is obvious that any experimental investigations pertaining to atom-laser outcoupling have to be performed for sufficiently short times

(i.e., for $t \ll t_c$) so that the coherence of the atom laser is guaranteed. In this context, mean-field theory has been shown capable of providing rather accurate and simple interpretation of the experimental observations (see, for instance, [20, 21, 22, 23]).

The presence of nonlinearities on the right-hand side of equations (11*a*)-(11*c*) complicates somewhat their solution. Nevertheless, as long as the continuum under consideration is smooth (i.e., slowly varying) it can be eliminated by means of standard approximations (e.g., pole approximation). The atomic density of states (8) can be considered as smooth only for frequencies well above ω_e and for sufficiently weak outcoupling rates. The latter assumption, however, is not always satisfied in typical experimental setups (e.g., see Ref. [22, 24]) and thus, the set of equations (11*a*)-(11*c*) has to be treated exactly.

To this end, we adopt here a uniform discretization approach. More precisely, we substitute the atomic continuum for frequencies within a range around $\omega_z/2$ (i.e., for $0 < \omega < \omega_{up}$), by a number (say M) of discrete modes, while the rest of the atom-mode density is treated perturbatively since it is far from resonance. The frequencies of the discrete modes are chosen to be $\omega_j = j\varepsilon$, where the mode spacing ε is determined by the upper-limit condition of the discretization, namely $\omega_{up} = M\varepsilon$. The corresponding coupling for the j mode, is determined by the spectral response (9) as follows $\tilde{g}_j^2 = D(\omega_j)\varepsilon$. Discussion on the choice of ω_{up} and the number of discrete modes can be found in Refs. [18]. Working as in [6], after the discretization equations (11*a*)-(11*c*) read,

$$\frac{\mathrm{d}\langle\hat{a}\rangle}{\mathrm{d}t} = -\mathrm{i}\left[\mu_A(t)/\hbar - S\right]\langle\hat{a}\rangle - \mathrm{i}(J - Se^{-\eta^2})\langle\hat{b}\rangle - \mathrm{i}\sum_{j=1}^{M}\tilde{g}_j\langle\hat{c}_j\rangle, \tag{12a}$$

$$\frac{\mathrm{d}\langle\hat{b}\rangle}{\mathrm{d}t} = -\mathrm{i}\left[\mu_B(t)/\hbar - Se^{-2\eta^2}\right]\langle\hat{b}\rangle - \mathrm{i}(J - Se^{-\eta^2})\langle\hat{a}\rangle - \mathrm{i}e^{-\eta^2}\sum_{j=1}^{M}\tilde{g}_j\langle\hat{c}_j\rangle, \tag{12b}$$

$$\frac{\mathrm{d}\langle\hat{c}_j\rangle}{\mathrm{d}t} = -\mathrm{i}\omega_j\langle\hat{c}_j\rangle - \mathrm{i}\tilde{g}_j\langle\hat{a}\rangle - \mathrm{i}\tilde{g}_j e^{-\eta^2}\langle\hat{b}\rangle, \tag{12c}$$

with the shift given by $S = \int_{\omega_{up}}^{\infty}\mathrm{d}\omega D(\omega)/\omega$, while we have introduced the chemical potentials for the two BECs namely, $\mu_A(t) = \hbar\omega_z/2 + 2\hbar\kappa|\langle\hat{a}(t)\rangle|^2$ and $\mu_B(t) = \hbar\omega_z/2 + 2\hbar\kappa|\langle\hat{b}(t)\rangle|^2$. In the absence of interactions, the time-dependent nonlinearities vanish and we recover the equations of motion for the interaction-free model of [7] with $\mu_A(t) = \mu_B(t) = \hbar\omega_z/2$.

4. Simulations

Throughout our simulations we have considered ^{23}Na BECs with $m = 3.818 \times 10^{-26}$ Kgr and $a_{tt} = 2.75 \times 10^{-9}$ m, which are formed independently in identical harmonic traps with longitudinal oscillation frequency $\omega_z = 200$ s^{-1} and ratio $\lambda = 0.4$. Condition (7) thus yields $N \ll 2.5 \times 10^3$ i.e., our two-mode model is valid for relatively small BECs consisting of a few hundred of atoms.

We assume that the BECs A and B are initially prepared in coherent states $|\alpha\rangle$ and $|\beta\rangle$, respectively. Equations (12*a*)-(12*c*) are thus solved with initial conditions

$$\begin{aligned}
&\langle\hat{a}(0)\rangle = \alpha = \sqrt{N\tilde{\alpha}(0)},\\
&\langle\hat{b}(0)\rangle = \beta = \sqrt{N\tilde{\beta}(0)}e^{\mathrm{i}\phi(0)},\\
&\langle\hat{c}_j(0)\rangle = 0,
\end{aligned} \tag{13}$$

where $\phi(0)$ is the initial relative phase between the two BECs. Accordingly, the initial number of condensed atoms in the traps A and B are given by $N_{\rm A}(0) = |\langle\hat{a}(0)\rangle|^2 = N\tilde{\alpha}(0)$ and $N_{\rm B}(0) = |\langle\hat{b}(0)\rangle|^2 = N\tilde{\beta}(0)$ respectively. Introducing the amplitude for the atomic continuum $\tilde{\gamma}$, at any time $t \geq 0$ we have $\tilde{\alpha}(t) + \tilde{\beta}(t) + \tilde{\gamma}(t) = 1$, so that $N_{\rm trap}(t) + N_{\rm C}(t) = N$, where $N_{\rm trap}(t) \equiv N_{\rm A}(t) + N_{\rm B}(t)$ and $N_{\rm C}(t)$ denote the population of the traps and continuum, respectively. Finally, for the sake of simplicity and without introducing any significant errors, the applied outcoupling pulse $\Lambda(t)$ is modeled as rectangular lasting from $t = 0$ to $t = \tau$. From now on, the indices A(B) and C, refer to traps A(B) and the continuum, respectively.

The dynamics of the system in the framework of an interaction-free model and for $\phi(0) = 0$ were analyzed in detail elsewhere [7]. For the sake of completeness, in the following subsection we recapitulate briefly the main results of [7].

4.1. Interaction-free model and vanishing relative phase

For the particular parameters under consideration, the weak-outcoupling regime corresponds to outcoupling rates $\Lambda < 5\times10^2$ s^{-2} [7]. In this regime, the system evolves in time with the BECs exchanging population but the oscillations are exponentially damped as atoms are irreversibly coupled out of the traps. The strength of the oscillations is determined by the Josephson coupling whereas the decay rate by the outcoupling strength Λ. Moreover, the distribution of the outcoupled atoms exhibits a characteristic asymmetric doublet with the two peaks separated by $2J$.

The strong-outcoupling regime occurs for $\Lambda \gtrsim 5 \times 10^2$ s^{-2} and is characterized by a continuous population exchange between the two BECs as well as between the BECs and the continuum. In the latter process, the pumping BEC seems to participate passively as its population is gradually transferred to the continuum in an irreversible way. On the contrary, the lasing BEC keeps exchanging population with the continuum even for larger times while for sufficiently strong outcoupling rates it is found only partially depleted in the long-time limit. The formation of such a bound state between the lasing condensate mode and the continuum is one of the most prominent effects associated with the non-Markovian nature of the dynamics. The distribution of the outcoupled atoms exhibits a broad peak, stemming from atoms directly outcoupled from the lasing BEC, while on the other hand atoms outcoupled from the pumping BEC give rise to a narrow peak. Most importantly, as a result of destructive quantum interference between the outcoupling channels in the system, the atomic distribution may also exhibit a dark spectral line (dip).

We turn now to the discussion of the dynamics of the system in the case of a non-vanishing initial relative phase between the two BECs, as well as in the presence of interatomic interactions.

4.2. Effects of relative phase

In order to understand the role of the initial relative phase $\phi(0)$, we solved equations $(12a)$-$(12c)$ numerically for increasing $\phi(0) \in [0, 2\pi]$. For the sake of comparison with the results presented in [7], throughout our simulations we have focused on an interaction-free model. Moreover, we have considered various outcoupling rates Λ, in order to cover both Markovian and non-Markovian dynamics. Nevertheless, before we proceed to such complicated simulations, it is worth recalling here that in the absence of atomic collisions and outcoupling (i.e., for $\kappa = 0$ and $\Lambda = 0$), the evolution of

the system is governed by the Josephson tunneling between the two BECs only. In this special case, the set of equations (12*a*)-(12*c*) can be easily solved analytically, obtaining for the trapped populations

$$\langle a^\dagger(t)a(t)\rangle = N_{\rm A}(0)\cos^2(Jt) + N_{\rm B}(0)\sin^2(Jt) + \sqrt{N_{\rm A}(0)N_{\rm B}(0)}\sin(2Jt)\sin[\phi(0)] \quad (14)$$

and $\langle b^\dagger(t)b(t)\rangle = N - \langle a^\dagger(t)a(t)\rangle$. The first two terms in equation (14), describe the population exchange between the two traps when initially $N_{\rm A}(0) \neq N_{\rm B}(0)$, whereas for $N_{\rm A}(0) = N_{\rm B}(0)$ the time evolution of the system is governed only by the third term which is proportional to $\sin[\phi(0)]$. This term describes interference phenomena between the two BECs [25] and was not present in the simulations performed in [7], as it vanishes for $\phi(0) = 0$. In the following, we discuss the atom laser dynamics for various values of $\phi(0)$.

4.2.1. Weak outcoupling—Markovian dynamics. In the weak-outcoupling regime, the damped oscillatory behavior of the trapped populations reflects the Josephson tunneling between the two BECs, and the irreversible outcoupling of atoms into the continuum. As shown in [7], the evolution of the system under both of these physical processes strongly depends on the trap separation as well as the frequencies and the outcoupling rates of the two condensate modes. In addition, the present simulations suggest a strong dependence on the initial relative phase between the two BECs, which affects mostly the exchange of atoms between them. As depicted in figure 1, the amplitude of the oscillations varies with $\phi(0)$, while in the case of $\phi(0) = \pi/2,\ 3\pi/2$ and for short times, a large fraction of the total population (more than 80%) may be found to occupy one of the traps only [see dashed and dotted lines in figures 1(a) and (b), respectively].

According to the inset of figure 1(a), the amplitude of the oscillations varies sinusoidally with $\phi(0)$; a behavior which can be explained, to some extent, in terms of the interference term appearing in equation (14), which is also proportional to $\sin[\phi(0)]$. Of course equation (14) has been derived in the framework of a particularly simple model pertaining to two isolated BECs, and as such cannot describe all aspects of the observed dynamics. For instance, it is obvious that the amplitude variation depicted in the inset of figure 1(a) is not symmetric around $\phi(0) = \pi$ while even the solutions we have obtained for $\phi(0) = 0$ and $\phi(0) = \pi$ do not coincide, despite the fact that the interference term in equation (14) vanishes in both cases. Such deviations from the perfect sinusoidal behavior can be attributed to the presence of the outcoupling mechanism which is not included in the simple model that equation (14) refers to. More precisely, in the present scenario the two condensate modes are not isolated, but rather coupled to the same continuum. As a result, we have various outcoupling channels for the system which may also interfere, thus giving rise to phenomena that cannot be described in the context of isolated BECs.

The distribution of the outcoupled atoms also varies with $\phi(0)$. More precisely, the characteristic doublet structure persists for any choice of $\phi(0)$, but the relative height of the peaks (ratio of the right to the left peak) changes periodically. For instance, in figure 2 we see that for $\phi(0) = 0$ (gray line), the right peak is more pronounced than the left peak, whereas the situation is the opposite for $\phi(0) = \pi$ (dashed line). Moreover, for $\phi(0) = \pi/2,\ 3\pi/2$ the two peaks have nearly the same heights (solid black line). For a better overview of this periodic change, in the inset of figure 2 we present the relative height of the two peaks for various values of $\phi(0)$ (stars). The observed behavior can be easily understood in terms of the global symmetric and

antisymmetric states $|\pm\rangle$ of the double-well potential [7]. The initial populations of the states are $P_\pm = |\sqrt{\tilde{\alpha}(0)} \pm \sqrt{\tilde{\beta}(0)}e^{i\phi(0)}|^2/2$ and thus their normalized ratio reads

$$\frac{P_+}{P_-} = \frac{1 + 2\sqrt{\tilde{\alpha}(0)\tilde{\beta}(0)}\cos[\phi(0)]}{1 - 2\sqrt{\tilde{\alpha}(0)\tilde{\beta}(0)}\cos[\phi(0)]}. \tag{15}$$

This expression describes the variation of the distribution of the initial population between the two global states with respect to $\phi(0)$. As depicted in the inset of figure 2, the ratio (15) (multiplied by a constant) is in a very good agreement with the periodic changes observed in the relative height of the two peaks in the distribution of the outcoupled atoms.

4.2.2. Strong outcoupling—Non-Markovian dynamics. Interference effects between the two BECs may also alter the evolution of the system in the strong outcoupling regime. More precisely, by varying the initial relative phase between the two BECs we find that the most noticeable changes in the evolution of the trapped populations occur for relatively short times, as well as in the long-time limit.

Let us start with trap B for which we can identify two distinct regimes in the evolution of the corresponding population for $\phi(0) = 0$ [see gray line in figure 3(b)]. For short times the main part of the population is transferred into the continuum. After this initial transient regime, dissipation is temporarily turned off and a weak oscillatory population exchange between the two traps sets in. Nevertheless, trap B is empty in the long-time limit as its population is gradually transferred into the continuum in an irreversible, almost exponential, way. As depicted in figure 3(b), the initial transient regime gradually disappears with increasing $\phi(0)$ and for $\phi(0) > 5\pi/6$, it is replaced by population exchange between the two BECs. In particular, for very short times the pumping BEC gets population from the lasing BEC, and this transfer becomes more pronounced as we increase $\phi(0)$ up to $\sim 4\pi/3$. After this initial population exchange, the condensate mode B decays almost exponentially and is empty in the long-time limit. Of course, increasing further $\phi(0) \in (4\pi/3, 2\pi]$, we find that the initial transient regime is gradually resettled.

The situation is similar but more interesting in the case of trap A. More precisely, as depicted in figure 3(a), the initial decay of the lasing condensate mode becomes faster and stronger as we increase $\phi(0)$ up to π. For $\phi(0) = 0$, the main part of the population that leaves the lasing BEC in this initial transient regime is lost into the continuum. The situation, however, is different for $\phi(0) \neq 0$ since only part of the population is outcoupled while the remaining part is transferred to trap B. This transfer becomes more pronounced for $\phi(0) > 5\pi/6$ [see black solid and dotted lines in figures 3(a,b)]. In any case, after this initial transient regime, dissipation is temporarily turned off and the condensate mode A exchanges population with the continuum only. This oscillatory population exchange persists even for longer times and the amplitude of the oscillations varies with $\phi(0)$. In the long-time limit, we have the formation of a bound state between the lasing condensate mode and the continuum. As a result, trap A exhibits a non-zero steady-state population which, as depicted in the inset of figure 3(a), also varies periodically with $\phi(0)$, and attains its maximum at $\phi(0) = \pi$. This behavior can be interpreted in terms of the global states $|\pm\rangle$ with energies $\omega_z/2 \pm J$. For $\eta < 2.0$, the Josephson coupling $J > 0$ and thus, the antisymmetric state $|-\rangle$ is closer to the edge than the symmetric state. As a

result, the antisymmetric state is more protected against dissipation and contributes the most to the steady-state population. Moreover, as we discussed earlier, the initial population of the antisymmetric state is given by $P_{-} = 0.5 - \sqrt{\tilde{\alpha}(0)\tilde{\beta}(0)}\cos[\phi(0)]$ and attains its maximum at $\phi(0) = \pi$. It is this periodic dependence of P_{-} on $\phi(0)$, that is also reflected in the steady-state population of trap A [see inset of figure 3(a)].

Finally, the choice of the initial relative phase may also affect significantly certain aspects of the distribution of outcoupled atoms in the strong-outcoupling regime. More precisely, the first aspect pertains to the relative height of the two peaks. As discussed in [7], the narrow peak stems from atoms directly outcoupled from the pumping BEC, whereas the broad peak is associated with atoms that emerge from the lasing BEC and as such experience stronger outcoupling. Thus, any variations in the population transfer between the two BECs with respect $\phi(0)$, are expected to be reflected in the relative height of the two peaks. Indeed, as discussed above, the fraction of the atoms transferred from the lasing to the pumping mode increases as we increase $\phi(0) \in [0, \pi]$. Accordingly, in this regime of relative phases the narrow peak related to the exponential decay of trap B becomes higher and more pronounced for increasing $\phi(0)$ at the detriment of the broad peak. Increasing $\phi(0)$ further, the narrow peak decreases again whereas the broad peak becomes stronger. The second aspect of the atomic distribution which is also of particular interest, involves the presence of a dark line (dip). As depicted in the inset of figure 4(a), the dip is present only $\phi(0) = 0$ or 2π, while a new dip appears between the two peaks for $\phi(0) = \pi$. These observations support the explanation for the dip given in [7] namely, it is a signature of destructive interference between the various outcoupling channels in the system. The degree as well as the nature of the interference is expected to vary with the relative phase between the two BECs. For instance, when $\Lambda = 5 \times 10^2 \mathrm{s}^{-2}$, the dip appears to give its place to a peak which is now a signature of constructive interference between various outcoupling channels [see figure 4(b)].

4.3. Effects of interatomic interactions

In general, the evolution of the system under consideration is governed by three distinct physical processes. More precisely, apart from the Josephson and the output coupling which were also present in the interaction-free model of [7], we also have the repulsive collisional interactions. It is reasonable therefore to define the ratios $\nu = \kappa N/J$ and $\xi = \kappa N/\sqrt{\Lambda}$ which quantify the effect of interatomic interactions relative to tunneling and outcoupling effects, respectively. How strongly the inclusion of interactions affects the results obtained in the framework of the interaction-free model of [7] depends on these two ratios. In particular, the largest deviations are expected for $\nu \gtrsim 1$ and $\xi \gtrsim 1$.

Before proceeding with our simulations, it is worth recalling here the dynamics of two isolated tunnel-coupled BECs [as determined by equations $(12a)$-$(12c)$ for $\Lambda = 0$]. In this case, the trapped population is conserved i.e., $N_{\mathrm{trap}}(t) = N$, while for a given initial population imbalance in the system $\tilde{p}(0) \equiv (N_{\mathrm{A}}(0) - N_{\mathrm{B}}(0))/N$, we have complete periodic oscillations between the two condensates (*Josephson regime*) [26] when [27]

$$H_{\mathrm{c}}(0) \equiv \frac{\nu}{2}\tilde{p}(0)^2 + \sqrt{1 - \tilde{p}(0)^2}\cos[\phi(0)] < 1. \tag{16}$$

The period of the oscillations increases with increasing nonlinearity (i.e., with increasing N) while the oscillations become anharmonic as $H_{\mathrm{c}}(0) \to 1$. Finally, for

$H_c(0) > 1$ the oscillations are no longer complete while their period reduces with increasing nonlinearity (*self-trapping regime*) [28].

One can readily check that $H_c(t)$ is a constant of motion in the absence of outcoupling. In our system, however, the situation is more involved as atoms are outcoupled from the two BECs with different rates and thus neither $N_{\rm trap}$ nor H_c is conserved. In the following, we discuss separately the dynamics of the system for weak and strong outcoupling rates when it starts from the Josephson and the self-trapping regime. As we will see, during its evolution the system may pass from one regime to the other.

4.3.1. Weak outcoupling—Markovian dynamics. In this subsection we investigate how the inclusion of interactions in our model affects the dynamics of the system in the weak-outcoupling regime. For the sake of comparison with the interaction-free model discussed in [7], we will focus on the case of vanishing initial relative phase between the two BECs.

When the system starts from the Josephson regime [i.e., if $H_c(0) < 1$] and $\nu < 1$, the evolution of the trapped populations in the presence of interactions is qualitatively similar to the evolution we obtained in the context of the interaction-free model. The small quantitative differences depicted in figure 5 are due to interatomic interactions which enter the equations of motion for $\langle\hat{a}(t)\rangle$ and $\langle\hat{b}(t)\rangle$ as time-dependent nonlinearities proportional to the corresponding trapped populations $N_{\rm A}(t) = |\langle\hat{a}(t)\rangle|^2$ and $N_{\rm B}(t) = |\langle\hat{b}(t)\rangle|^2$ [see equations (12*a*) and (12*b*)]. As a result, the chemical potentials of the two BECs fluctuate in time and become off-resonant. As long as $\nu < 1$ the nonlinearities are so weak that may only shift the oscillations in the populations with respect to the oscillations in the case of the ideal gas, whereas for $\nu \gtrsim 1$ the nonlinearities are sufficiently strong to disturb the exchange of population between the two BECs. In particular, as is evident in figure 6, the oscillatory behavior of both occupation probabilities becomes less pronounced as we increase the nonlinearity in the system. Thus for sufficiently strong nonlinearities the two traps tend to decay nearly exponentially into the atomic continuum (see solid curves in figure 6).

The question that arises here is whether the system remains in the Josephson regime throughout its evolution or not. To answer this question, one may follow, for instance, the time evolution of $H_c(t)$ [with $\nu = \kappa N_{\rm trap}(t)/J$, $\tilde{p}(t) \equiv (N_{\rm A}(t) - N_{\rm B}(t))/N$, $\phi(t) = \arg(\langle a^\dagger b\rangle)$] which is not a conserved quantity anymore, as atoms are continuously coupled out of the traps. In figure 7 we plot the evolution of $H_c(t)$ as a function of time, for the parameters of figure 5(a) (with $N = 50$). Clearly, we have $H_c(t) < 1$ for all t, and thus we may safely conclude that the system remains in the Josephson regime throughout its evolution. The same conclusion can be drawn by following the evolution of $H_c(t)$ for the parameters of the other plots in figures 5 and 6

Let us consider now the situation where the system starts from the self-trapping regime [i.e., $H_c(0) > 1$] . As depicted in figure 8, for short-times the occupation probabilities for the two traps undergo partial oscillations which typically characterize the self-trapping regime. Gradually, however, the population imbalance between the two traps reduces as atoms are coupled out of trap A, e^{η^2} times faster than trap B and after some time we have $N_{\rm A} = N_{\rm B}$ (vertical gray lines). In the absence of losses (i.e., for $\Lambda = 0$) such a balanced state can be a stationary state of the nonlinear Schrödinger equation. In the present case, however, the system is driven again away

from this state as the outcoupling mechanism is still on and the population balance is immediately destroyed. For sufficiently weak nonlinearities, the balanced state marks the transition from the self-trapping to the Josephson regime where we have complete damped oscillations between the two traps [e.g., see figures 8(b,c)]. On the contrary, for larger nonlinearities [see figure 8(d)], the system tends to continue in the self-trapping regime up to the point the population imbalance between the two traps vanishes again. These transitions are also evident in the evolution of the corresponding $H_{\rm c}(t)$, presented in figure 7(b). In contrast to figure 7(a), we see here that $H_{\rm c}(t)$ exhibits abrupt and instantaneous changes, which of course are not reflected in the evolution of the corresponding populations. However, the profile of $H_{\rm c}(t)$ (thick line) characterizes rather accurately the transition points discussed above.

According to our simulations, the ratio ξ does not seem to affect considerably the oscillatory behavior of the occupation probabilities for the two traps. This was to be expected to some extent, as we are in the weak-outcoupling regime and thus these oscillations reflect the population exchange between the two BECs. Hence, it is the ratio ν the one that determines how strongly the population exchange is affected by the presence of interactions in the system. Nevertheless, our simulations show that the distribution of the outcoupled atoms is determined by the ratio ξ.

In figure 9 we depict the distribution of outcoupled atoms at $\tau = 10$ s for various atom numbers, and let us focus for a while on the upper peak of the doublet. As we increase the number of atoms in the system, the peak becomes broader while its shape starts deviating from the standard Lorentzian profile. Actually, for $\xi \gtrsim 1$ it acquires a rather complicated structure. This behavior can be understood in terms of the time-dependent chemical potentials appearing in equations (12*a*) and (12*b*). More precisely, due to the applied outcoupling mechanism, the trapped population reduces with time. For very short times, the frequency of the outcoupled atoms that contribute to the upper peak is roughly $\mu_{\rm A}(0)/\hbar + J$ while as time goes on, $\mu_{\rm A}(t)$ changes due to the applied outcoupling mechanism as well as the coupling to the pumping condensate. Hence, outcoupled atoms may involve different frequencies and the center of the atomic distribution is shifted accordingly towards lower or upper frequencies ("chirping"); a phenomenon which is reflected in the broadening of the upper peak. Moreover, interference effects between atoms which have the same frequency and were outcoupled at different times, may also give rise to unconventional atomic distributions exhibiting multiple spikes [see figures 9(c-d)].

Increasing the total number of atoms in the system N or reducing the outcoupling rate $\sqrt{\Lambda}$, we essentially increase the ratio ξ and thus the effects of interactions on the atom-laser outcoupling are more pronounced. In this spirit one may notice, for example, that the same interaction effects we have just described also appear on the lower peak, albeit sooner. The reason is simply that this peak is associated with atoms outcoupled directly from trap B with outcoupling rate $\sqrt{\Lambda}e^{-\eta^2}$.

In closing, we would like to point out that similar conclusions can be drawn by following the evolution of the atomic distribution with time, for a fixed initial nonlinearity i.e., for a given N. In this case, the effects of interactions become more prominent as time goes on, and the distribution of the outcoupled atoms begins exhibiting sharp spikes due to quantum interference. Moreover, all atomic distributions we have checked throughout our simulations show the characteristics discussed above, irrespective of the chosen initial conditions. Finally, it is worth noting that the "chirping" effect and the unconventional atom laser spectra have also been predicted recently by Johnsson *et al.* [20], and a chirp-compensation mechanism

has been proposed. Moreover, chirping effects may also occur in more realistic three-dimensional systems, disturbing the transverse density distribution of the atom-laser beam [21].

4.3.2. Strong outcoupling—Non-Markovian dynamics. We turn now to the discussion of how the inclusion of interactions in our model affects the evolution of the system and the distribution of outcoupled atoms in the strong-outcoupling regime. As in the weak-outcoupling regime, we will focus on $\phi(0) = 0$.

In figures 10 and 11, we plot the evolution of the occupation probabilities for the traps as functions of time. The gray curve refers to an interaction-free model whereas the other two curves have been obtained for a weakly interacting gas when the system starts from the Josephson and the self-trapping regime. In any case, when $\xi < 1$ we may note only small deviations from the interaction-free model (see figure 10). The reason is that in the strong-outcoupling regime the evolution of the system is mainly governed by the exchange of population between the BECs and the continuum. Thus, as long as $\xi < 1$, the effect of interactions on the evolution of the system is negligible, whereas when the system starts from the self-trapping regime and $\xi \gtrsim 1$, we note large deviations from the interaction-free model (see black solid line in figure 11). Moreover, for $N = 100$ and the parameters of figure 10, $H_c(t) < 1$ for all times, and thus the system remains in the Josephson regime throughout its evolution. On the contrary, for $N = 200$, as well as for the parameters of figure 11, a transition from the self-trapping to the Josephson regime occurs rather soon i.e., at $t \approx 9 - 13$ ms.

Our simulations also show a decrease of the steady-state population of trap A which is associated with the formation of a bound state between the lasing condensate mode and the continuum. The destruction of the bound state is due to the repulsive character of the interactions and has been predicted earlier by many authors in the context of the single-mode model [1, 5]. Here, however, we see that the same phenomenon also persists in the two-mode model under consideration while, as depicted in the inset of figure 10(a), the drop of the steady-state population for increasing atom numbers can be considered as linear to a good accuracy.

The effect of interactions on the distribution of outcoupled atoms in the strong-outcoupling regime is summarized in figures 12. For relatively weak nonlinearities (i.e., for $\xi < 1$) the distribution of the outcoupled atoms keeps all the main features noted in the interaction-free model [see figures 12(a-b)]. The atomic distributions are mostly affected by the presence of interactions when $\xi \gtrsim 1$ [see 12(c-d)]. In this case the chirping effect sets in and the distribution becomes broader. Moreover, quantum interference between atoms which have the same frequency but were outcoupled at different times may give rise to rich patterns involving multiple peaks and dips. Nevertheless, in contrast to the weak-outcoupling regime discussed earlier, these peaks (dips) are broader in the present case due to the strong outcoupling rates (compare to figure 9).

Finally, we would like to emphasize once more that the origin of the dips in the atomic distribution of figure 12(c), is completely different from the one of the dark spectral line predicted in [7]. More precisely, as discussed earlier, the multiple dips depicted in figure 12(c) stem from the interference between atoms which have the same energy but were outcoupled at different times (i.e., they have different phases). Interference patterns of this type are not expected to depend considerably on the choice of the initial relative phase between the two BECs, and thus they are present for any choice of $\phi(0)$. On the contrary, the dark line predicted in [7] is a signature of perfectly

destructive quantum interference between different outcoupling channels in the system. This fact was also confirmed in section 4.2.2, where we showed that the dark line is perfect only for $\phi = 0,$ and 2π. Moreover, as shown in figure 12(e), interactions also tend to disturb the interference phenomena between various outcoupling channels and thus the dark spectral line is not perfect for $\kappa \neq 0$. From the mathematical point of view, this is due to the time-dependent nonlinearities which render the two condensate modes off-resonant as well as the repulsive nature of the interactions.

5. Conclusions

Using a two-mode model, we have studied aspects of the dynamics of a continuous atom laser based on the merging of independently formed BECs. In particular, we examined effects of interatomic interactions and the role of the relative phase between the two BECs on the evolution of the trapped populations and the distribution of outcoupled atoms. Our simulations were performed in the weak- and the strong-outcoupling regimes.

For the sake of comparison to earlier work [7], we studied the role of the relative phase in the framework of an interaction-free system, and showed that it affects considerably the exchange of population between the two BECs, as well as the fraction of the population which remains trapped in the long-time limit for strong outcoupling rates. The distribution of outcoupled atoms exhibits always a characteristic doublet, with the phase determining the relative height of the two peaks. Moreover, quantum interference between various outcoupling channels in the system, may give rise to new peaks or even dark spectral lines in the distribution of outcoupled atoms. All of these phenomena, and in particular the unconventional form of the spectrum, stem from the presence of the pumping BEC in the neighborhood of the lasing condensate. More precisely, as long as the outcoupling mechanism is always on during the merging process, the transported BEC is also expected to interact with the applied electromagnetic radiation before the completion of the merging.

In the absence of interactions the energies of the lasing and the pumping condensates are constant, whereas in the presence of interactions the two condensates are characterized by their chemical potentials, which depend on the number of trapped atoms. Hence, both of the potentials change as atoms are transferred from one condensate mode to the other, but mainly due to the applied outcoupling mechanism which affects differently the population of the two condensates. The two condensate modes become thus off-resonant, and this affects mostly the population exchange between the two modes. Of course, the most noticeable changes occur for nonlinearities whose strength is at least comparable to the outcoupling rate and/or the Josephson coupling. Moreover, for sufficiently strong interactions macroscopic quantum self-trapping may occur, where the population transfer from one mode to the other is partially turned off. This is a nonlinear effect arising from the interatomic interactions, and is preserved in time when the double-well system is isolated. In the present case, however, the presence of outcoupling affects the trapped populations and the relative phase between the two BECs, causing the system to enter gradually the Josephson regime, where it remains for the rest of its evolution. In the strong-outcoupling regime interatomic interactions seem to prevent the formation of a bound state between the lasing mode and the continuum. In particular, our simulations show that the steady-state trapped population decreases linearly with increasing strength of the nonlinearity.

Finally, the variation of the chemical potential of the lasing condensate with time is also reflected in the spectrum of the atom laser, as the outcoupled atoms experience a time-dependent mean-field potential, and thus their energy also varies over time (chirping). This effect causes a significant broadening of the distribution of outcoupled atoms, which may also exhibit complicated patterns reflecting the interference between atoms which have the same energy but were outcoupled at different time instants. Reducing the effect of the mean-field potential on the outcoupled atoms (e.g., by reducing the condensate density or working with interaction-free BEC systems in the vicinity of Fesbach resonances) one may in general improve the spectrum of the atom laser. It is worth noting, however, that an ideal continuous atoms laser working at steady state is not expected to suffer by chirping effects as the population of the lasing mode is kept constant.

Acknowledgments

The work of GMN and PL was supported in part by the EC RTN EMALI (contract No. MRTN-CT-2006-035369).

References

[1] Moy G M, Hope J J and Savage C M 1999 *Phys. Rev. A* **59** 667
[2] Hope J J, Moy G M, Collett M J and Savage C M 2000 *Phys. Rev. A* **61** 023603
[3] Jack M W, Naraschewski M , Collett M J and Walls D F 1999 *Phys. Rev. A* **59** 2962
[4] Breuer H P, Faller D, Kappler B and Petruccione F 1999 *Phys. Rev. A* **60** 3188
[5] Jeffers J, Horak P, Barnett S M and Randmore P M 2000 *Phys. Rev. A* **62** 043602
[6] Nikolopoulos G M, Lambropoulos P and Proukakis N P 2003 *J. Phys. B: At. Mol. Opt. Phys.* **36**, 2797
[7] Lazarou C, Nikolopoulos G M, and Lambropoulos P 2007 *J. Phys. B: At. Mol. Opt. Phys.* **40** 2511
[8] Chikkatur A P, Shin Y, Leanhardt A E, Kielpinski D, Tsikata E, Gistavson T L, Pitchard D E and Ketterle W 2003 *Science* **282** 2193
[9] Yi W and Duan L-M 2005 *Phys. Rev. A* **71** 043607
[10] Mebrahtu A, Sanpera A and Lewenstein M 2006 *Phys. Rev. A* **73** 033601
[11] Meystre P 2001 *Atom Optics* (New York: Springer Verlag)
[12] Moy G M, Hope J J and Savage C M 1997 *Phys. Rev. A* **55** 3631
[13] Guerin W, Riou J-F, Gaebler J P, Josse V, Bouyer P and Aspect A 2006 *Phys. Rev. Lett.* **97** 200402
[14] Javanainen J and Ivanov M Y 1999 *Phys. Rev. A* **60** 2351; Milburn G J, Corney J, Wright E M and Walls W F 1997 *Phys. Rev. A* **55** 4318
[15] Strunz W T, Diosi L and Gisin N 1999 *Phys. Rev. Lett* **82** 1801; Diosi L, Gisin N and Strunz W T 1998 *Phys. Rev. A* **58** 1699 (1998)
[16] Garraway B M 1997 *Phys. Rev. A* **55** 2290; Dalton B J, Barnett S M, and Garraway B M 2001 *Phys. Rev. A* **64** 053813
[17] Jack M W and Hope J J 2001 *Phys. Rev. A* **63** 043803
[18] Nikolopoulos G M, Bay S and Lambropoulos P 1999 *Phys. Rev. A* **60** 5079; Nikolopoulos G M and Lambropoulos P 2000 *Phys. Rev. A* **61** 053812
[19] Imamoglu A, Lewenstein M, and You L 1997 *Phys. Rev. Lett.* **78** 2511
[20] Johnsson M, Haine S, Hope J, Robins N, Figl C, Jeppesen M, Dugué J, and Close J 2007 *Phys. Rev. A* **75**, 043618
[21] Riou J-F, Guerin W, Le Coq Y, Fauquembergue M, Josse V, Bouyer P, and Aspect A 2006 *Phys. Rev. Lett.* **96** 070404; Köhl M, Busch T, Mølmer K, Hänsch T W, and Esslinger T 2005 *Phys. Rev. A* **72** 063618; Busch T, Köhl M, Esslinger T, Mølmer K 2002 *Phys. Rev. A* **65**, 043615
[22] Robins N P, Morrison A K, Hope J J and Close J D 2005 *Phys. Rev. A* **72** 031606(R)
[23] Schneider J and Schenzle A 1999 *Appl. Phys. B* **69** 353; Steck H, Naraschewski M and Wallis H 1998 *Phys. Rev. Lett.* **80** 1; Graham R and Walls D F 1999 *Phys. Rev. A* **60** 1429

[24] Mews M-O, Andrews M R, Kurn D M, Durfee D S, Townsend C G and Ketterle W 1997 *Phys. Rev. Lett.* **78** 582
[25] Andrews M R, Townsend C G, Miesner H-J, Durfee D S, Kurn D M, and Ketterle W 1997 *Science* **275** 637 ; Javanainen J and Yoo M 1996 *Phys. Rev. Lett.* **76** 161
[26] Javanainen J 1986 *Phys. Rev. Lett.* **57** 3164
[27] Raghavan S, Smerzi A, Fantoni S, ans Shenoy S R 1999 *Phys. Rev. A* **59** 620
[28] Albiez M, Gati R, Fölling J, Hunsmann S, Cristani M and Markus M K 2005 *Phys. Rev. Lett.* **95** 010402; Smerzi A, Fantoni S, Giovanazzi S and Shenoy S R 1997 *Phys. Rev. Lett.* **79** 4950

Figure captions

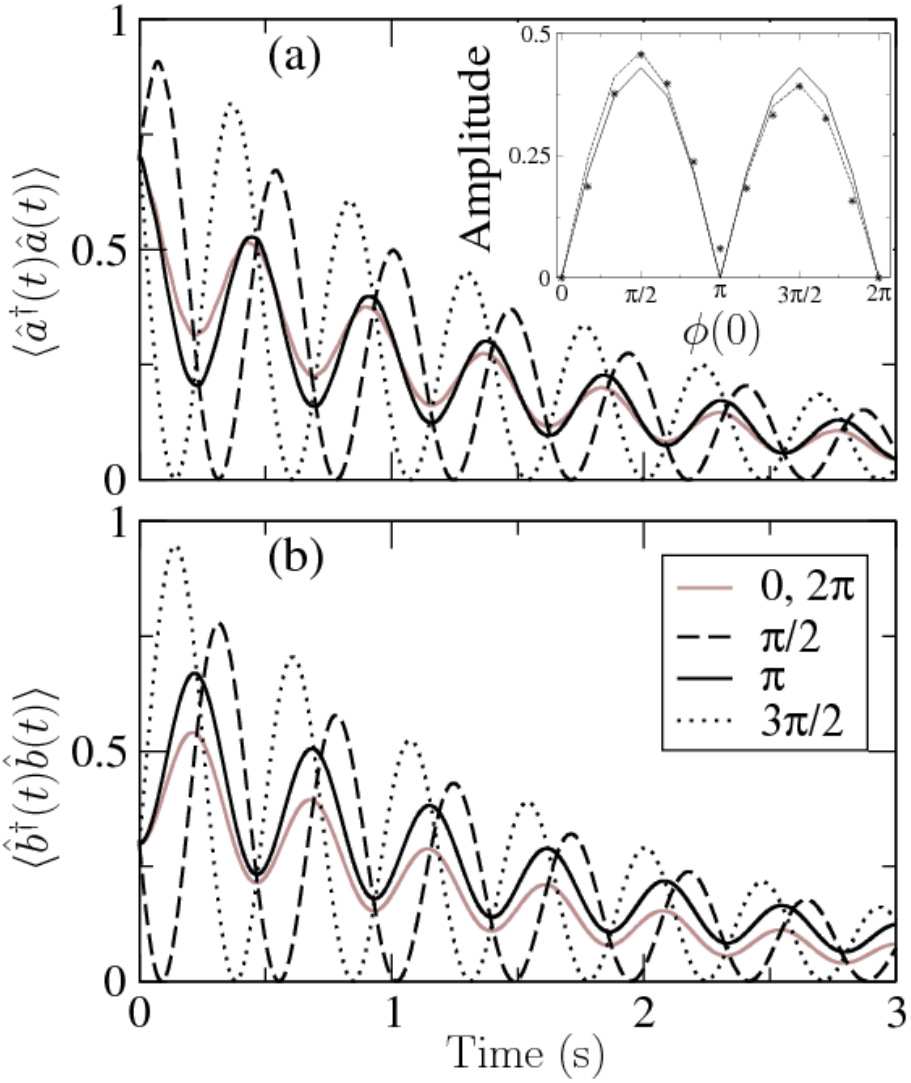

Figure 1. Effects of the relative phase on the Markovian dynamics. The normalized trapped populations are plotted as functions of time for various values of the initial relative phase $\phi(0)$ between the two BECs. Inset: Typical behavior of the amplitude of the oscillations for varying initial relative phase $\phi(0)$. The depicted values (stars) are estimated from the evolution of the trapped population $|\langle \hat{a}^\dagger(t)\hat{a}(t)\rangle|^2$ for various $\phi(0)$ and in particular at its second peak. The corresponding amplitude for $\phi(0) = 0$ is used as a reference amplitude. The solid and the dashed lines are sinusoidal fitting to the data, with constant ($\sim |\sin[\phi(0)]|$) and exponentially damped amplitude ($\sim |\sin[\phi(0)]|e^{-0.05\phi(0)}$), respectively. Parameters: $\omega_z = 200$ s^{-1}, $\kappa = 0$, $\lambda = 0.4$, $\Lambda = 10^2$ s^{-2}, and $\eta = 1.7$. Initial conditions: $\tilde{\alpha}(0) = 0.7$, $\tilde{\beta}(0) = 0.3$. Discretization parameters: $M = 1500$, $\omega_{\rm up} = 300$ s^{-1}.

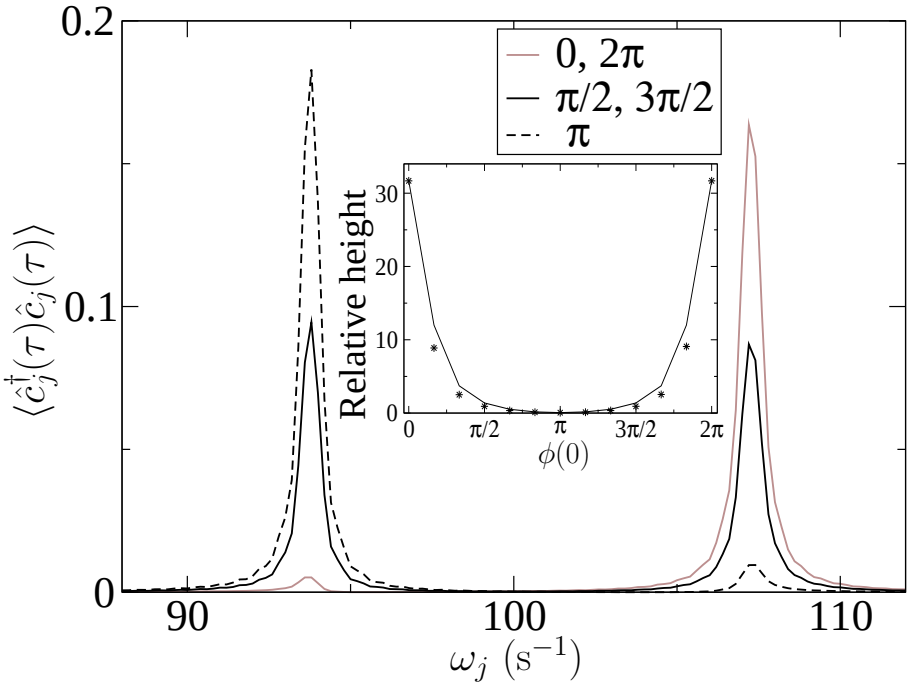

Figure 2. Effects of the relative phase on the distribution of outcoupled atoms in the Markovian regime. The distributions have been obtained at $\tau = 10$ s for various values of the initial relative phase $\phi(0)$ between the two BECs. Inset: Typical behavior of the relative height of the two peaks (ratio of the right to the left) for varying initial relative phase $\phi(0)$. The depicted values (stars) are estimated from the atomic distributions at $\tau = 10$ s for various $\phi(0)$. The solid line is a fitting to the data according to ratio (15). Parameters as in figure 1.

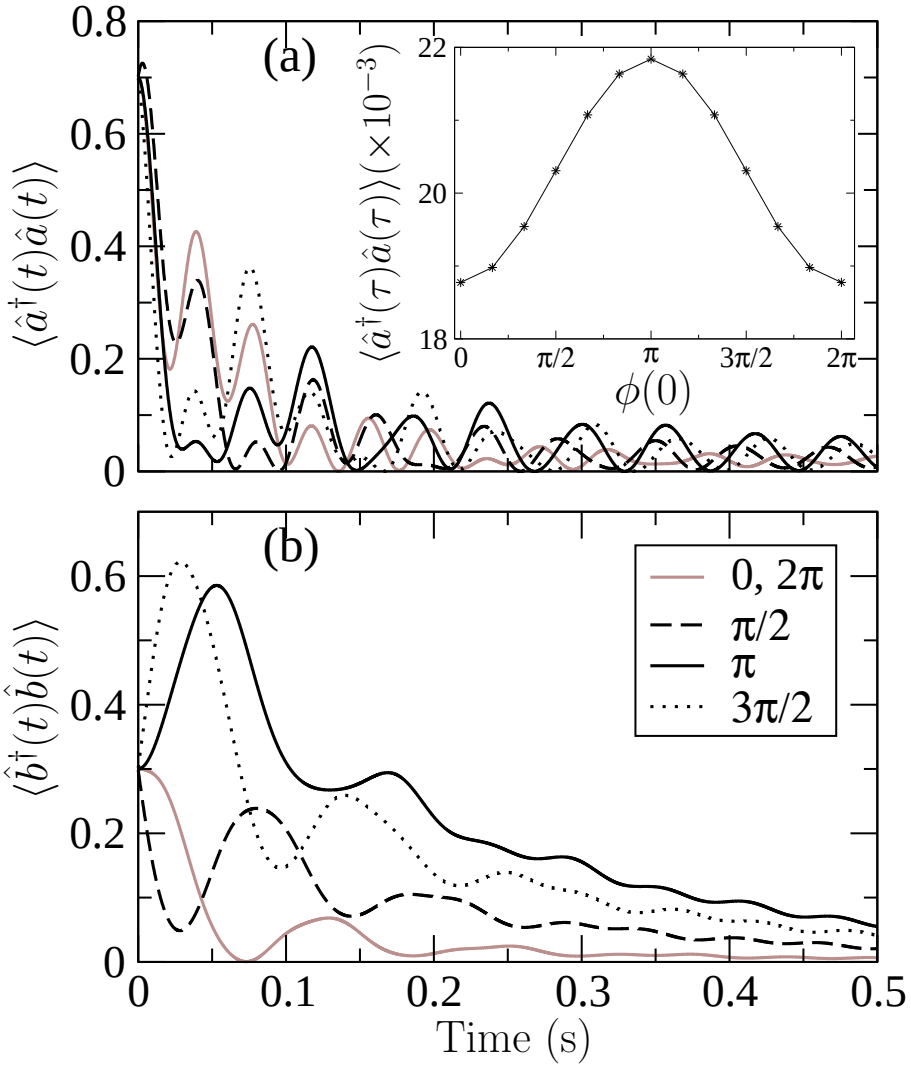

Figure 3. Effects of the relative phase on the non-Markovian dynamics. The normalized trapped populations are plotted as functions of time for various values of the initial relative phase $\phi(0)$ between the two BECs. Inset: Typical behavior of the steady-state population of the lasing condensate mode for varying initial relative phase between the two BECs. The depicted values (stars) are estimated numerically at $\tau = 10$ s, whereas the solid line is a fitting of the form $x+y\cos[\phi(0)]$. Parameters: $\omega_z = 200$ s^{-1}, $\kappa = 0$, $\lambda = 0.4$, $\Lambda = 4 \times 10^3$ s^{-2}, and $\eta = 1.5$. Initial conditions: $\tilde{\alpha}(0) = 0.7$, $\tilde{\beta}(0) = 0.3$. Discretization parameters: $M = 1500$, $\omega_{\rm up} = 300$ s^{-1}.

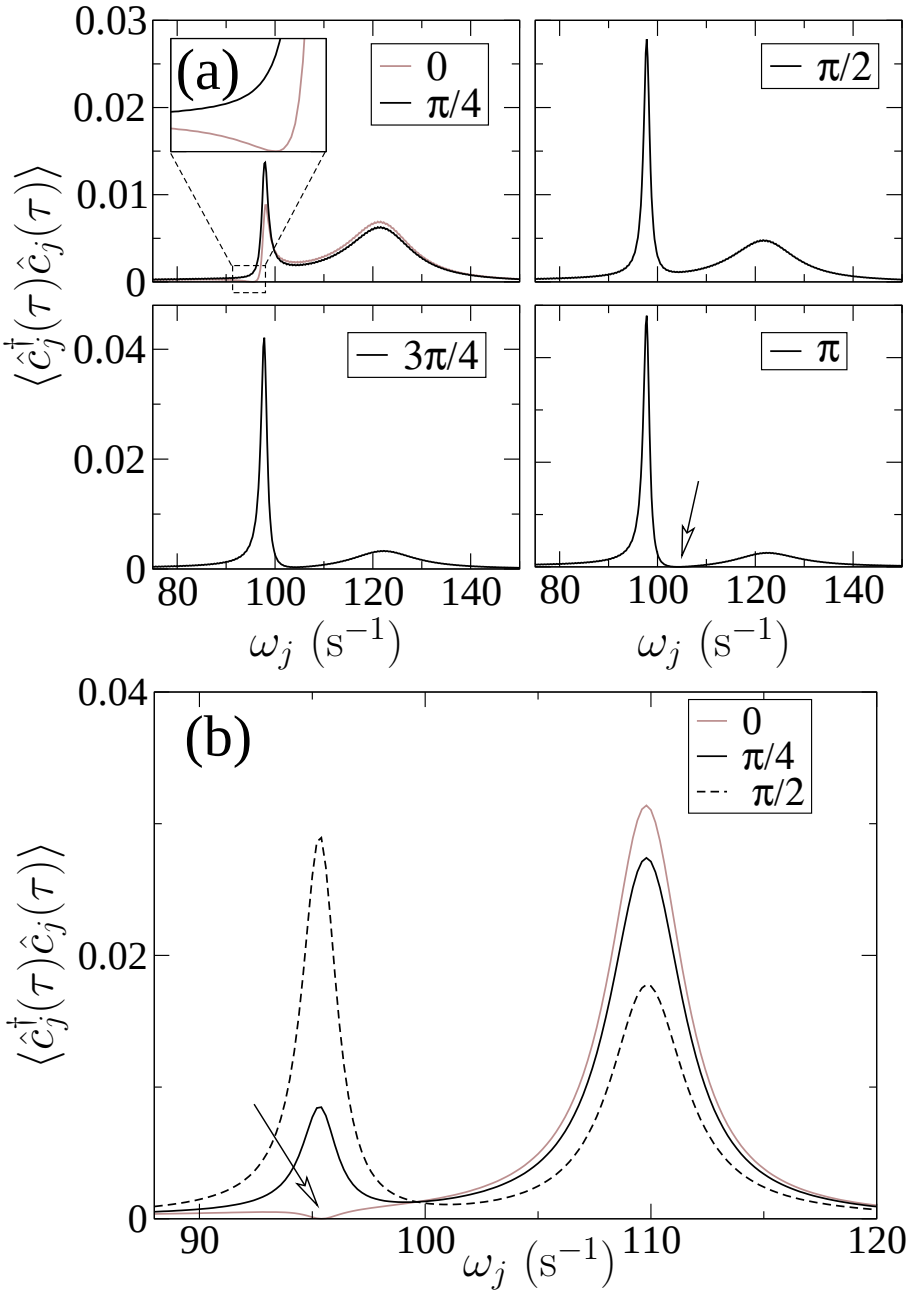

Figure 4. Effects of the relative phase on the distribution of outcoupled atoms in the non-Markovian regime. The distributions have been obtained at $\tau = 10$ s for various initial values of the relative phase $\phi(0)$ between the two BECs. Other parameters as in figure 3, but for $\eta = 1.7$ and $\Lambda = 2 \times 10^3$ s^{-2} (a); $\eta = 1.7$ and $\Lambda = 5 \times 10^2$ s^{-2} (b). The arrows point at the dips while the inset shows a closeup of the atomic distribution around it.

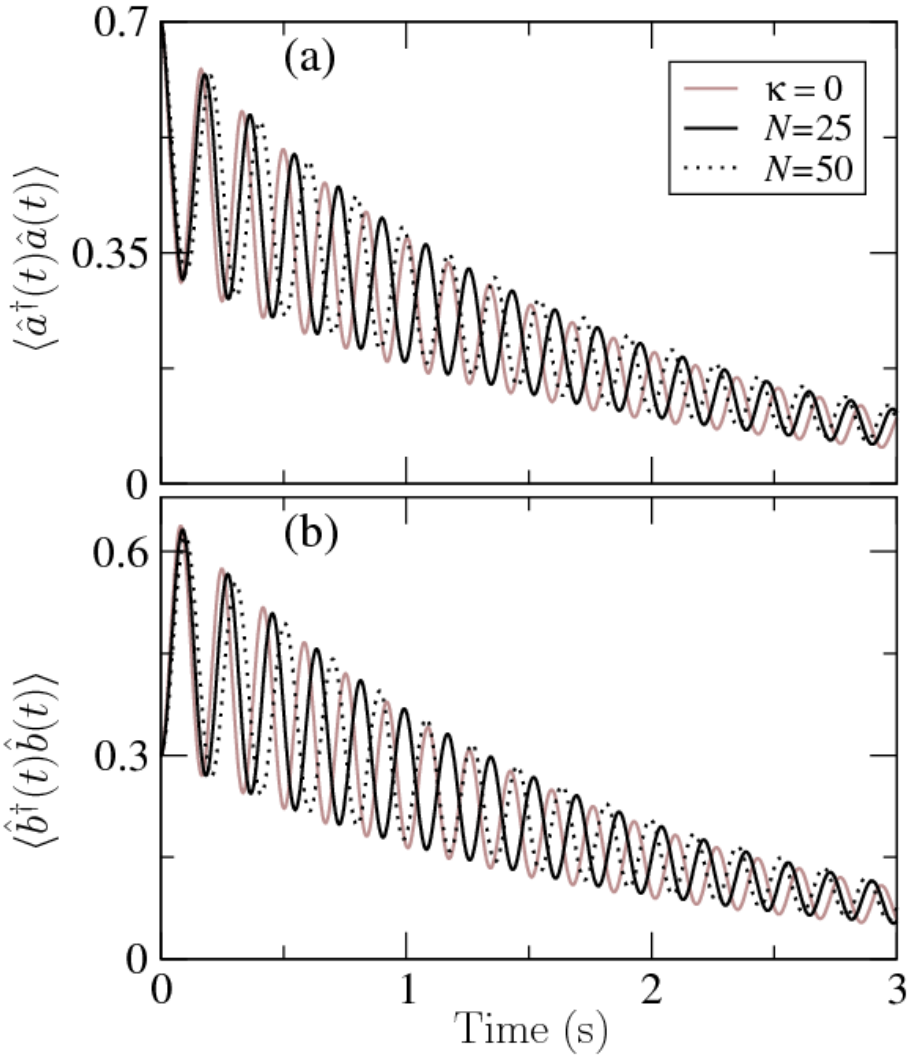

Figure 5. Effects of interatomic interactions on the Markovian dynamics. The normalized trap populations are plotted as functions of time for various atom numbers and $\omega_z = 200\ \mathrm{s}^{-1}$, $\lambda = 0.4$, $\Lambda = 10^2\ \mathrm{s}^{-2}$, and $\eta = 1.5$. The gray curves correspond to an interaction-free Bose gas. Initial conditions: Josephson regime with $\tilde{\alpha}(0) = 0.7$, $\tilde{\beta}(0) = 0.3$, $\phi(0) = 0$. Discretization parameters: $M = 1500$, $\omega_{\mathrm{up}} = 300\ \mathrm{s}^{-1}$.

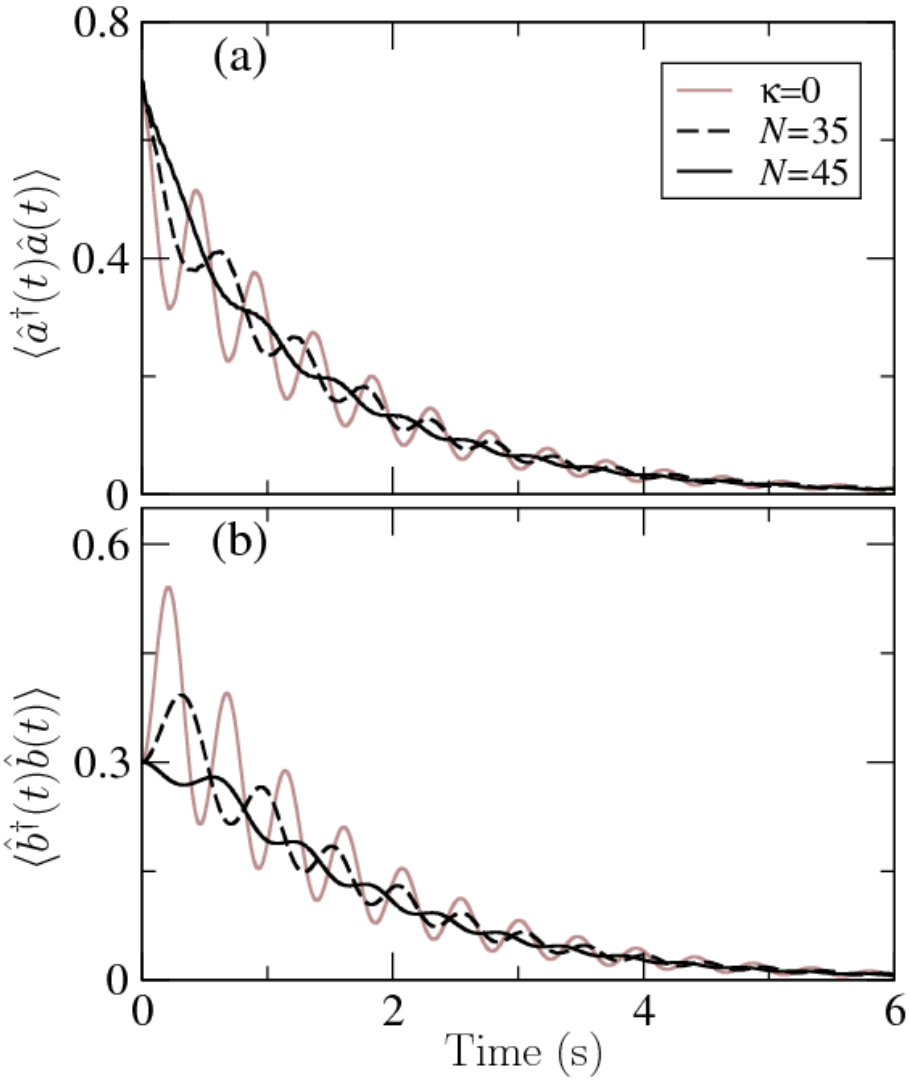

Figure 6. As in figure 5 for $\eta = 1.7$.

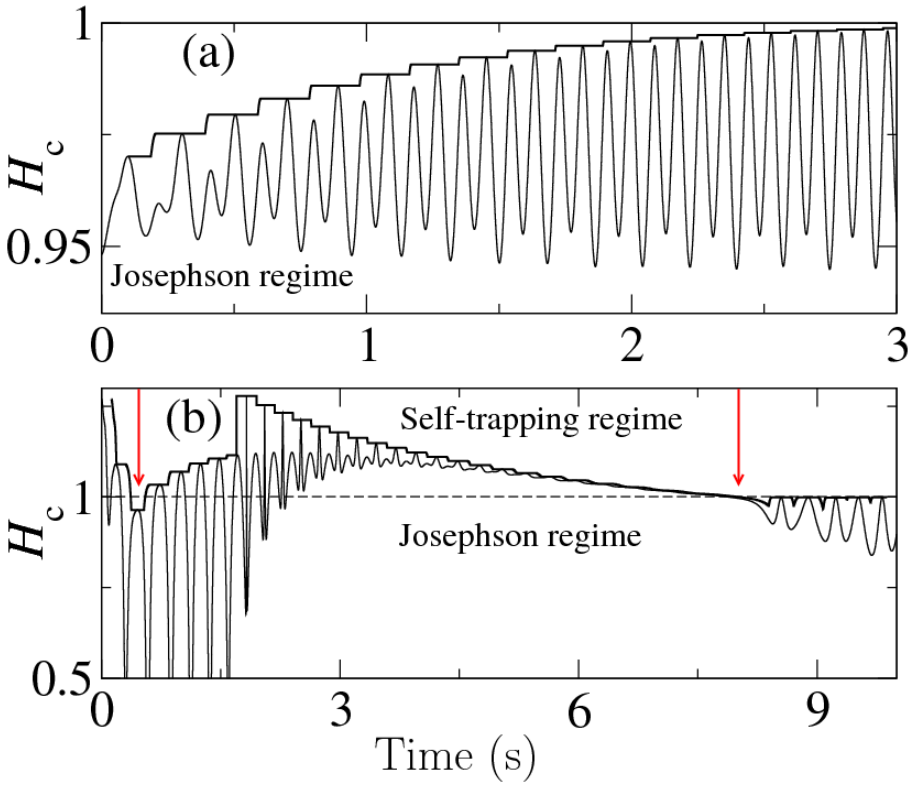

Figure 7. The evolution of H_c (thin line) and its envelope (thick line), are plotted as functions of time for the parameters of figure 5(a) ($N = 50$) and figure 8(d). The arrows point at the regions where the system passes from one regime to the other.

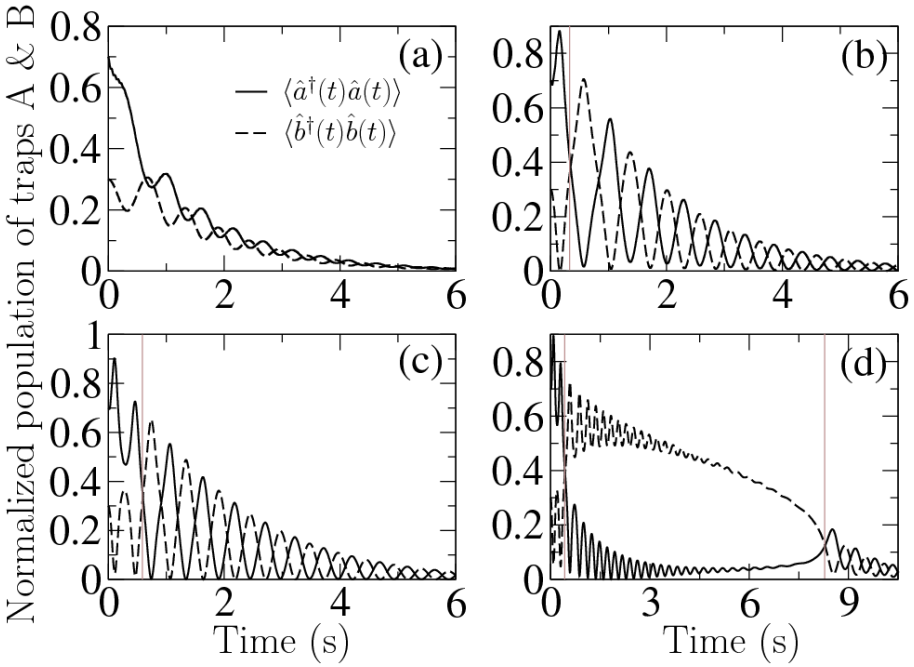

Figure 8. Effects of interatomic interactions on the Markovian dynamics. The normalized trap populations are plotted as functions of time for various atom numbers: (a) $N = 50$; (b) $N = 100$; (c) $N = 150$; (d) $N = 200$. The vertical gray line denotes the border between self-trapping and Josephson regime. Parameters: $\omega_z = 200\ \mathrm{s}^{-1}$, $\lambda = 0.4$, $\Lambda = 10^2\ \mathrm{s}^{-2}$, $\eta = 1.7$. Initial conditions: self-trapping regime with $\tilde{\alpha}(0) = 0.7$, $\tilde{\beta}(0) = 0.3$, $\phi(0) = 0$. Discretization parameters: $M = 1500$, $\omega_{\mathrm{up}} = 300\ \mathrm{s}^{-1}$.

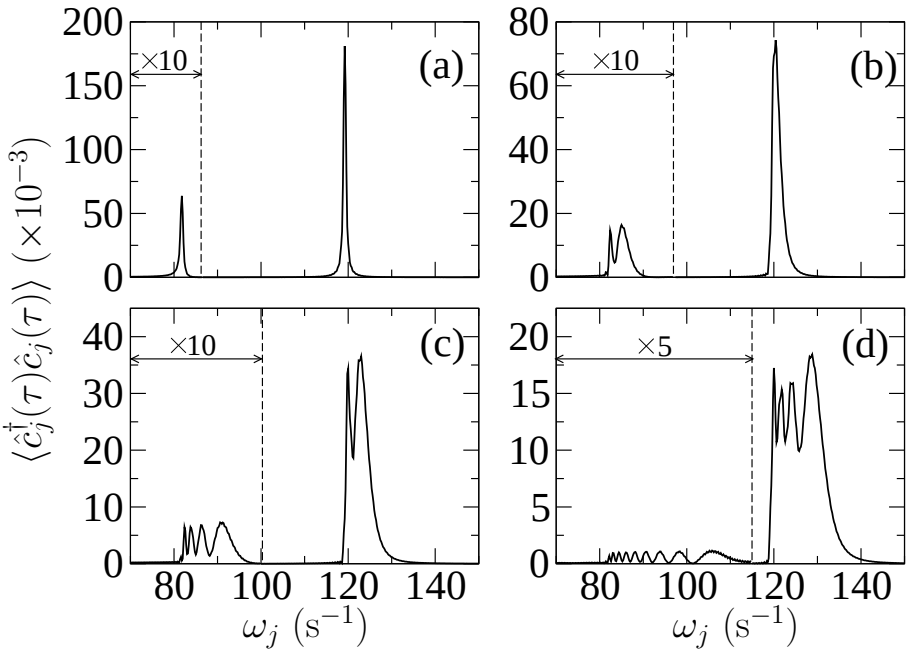

Figure 9. Effects of interatomic interactions on the distribution of outcoupled atoms in the Markovian regime. The distribution (a) corresponds to an interaction-free Bose gas whereas the other three distributions have been obtained for a weakly interacting Bose gas with $N = 25$ (b), $N = 50$ (c), $N = 100$ (d). Parameters: $\omega_z = 200$ s^{-1}, $\lambda = 0.4$, $\Lambda = 10^2$ s^{-2}, $\eta = 1.5$, $\tau = 10$ s. Initial conditions: Josephson regime with $\tilde{\alpha}(0) = 0.7$, $\tilde{\beta}(0) = 0.3$, $\phi(0) = 0$. Discretization parameters: $M = 1500$, $\omega_{\mathrm{up}} = 300$ s^{-1}.

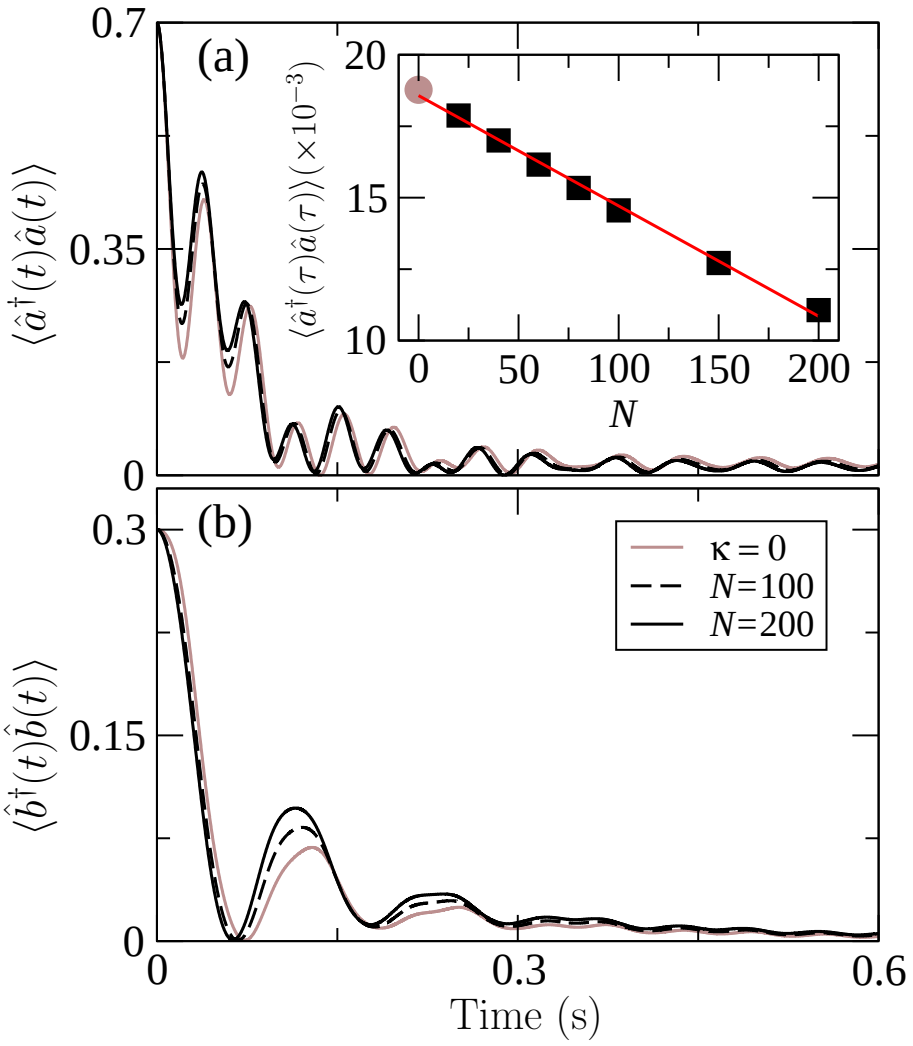

Figure 10. Effects of interatomic interactions on the non-Markovian dynamics. The normalized trap populations are plotted as functions of time for $\omega_z = 200\ \mathrm{s}^{-1}$, $\lambda = 0.4$, $\Lambda = 4 \times 10^3\ \mathrm{s}^{-2}$, $\eta = 1.5$. The inset shows the typical behavior of the steady-state population of trap A at $\tau = 10$ s for various atom numbers. The gray curves and circles correspond to an interaction-free Bose gas. Initial conditions: Josephson regime ($N = 100$) and self-trapping regime ($N = 200$) with $\tilde{\alpha}(0) = 0.7$, $\tilde{\beta}(0) = 0.3$, $\phi(0) = 0$. Discretization parameters: $M = 1500$, $\omega_{\mathrm{up}} = 300\ \mathrm{s}^{-1}$.

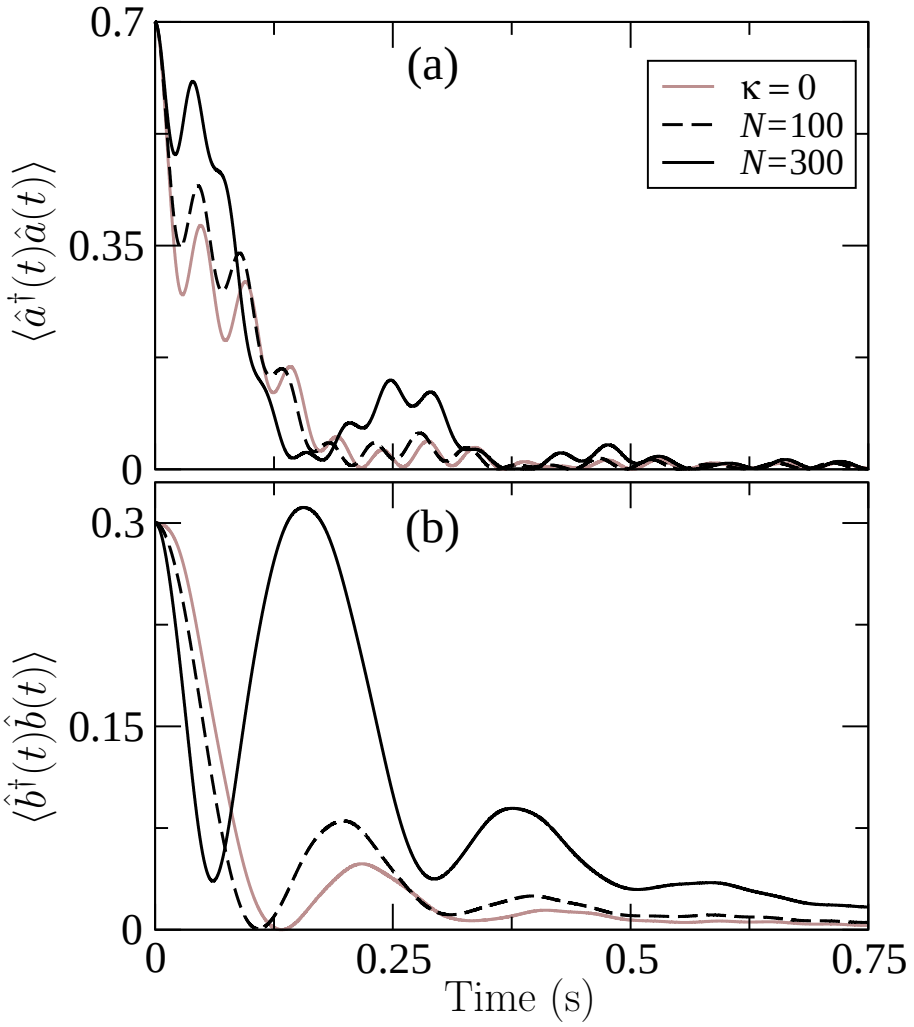

Figure 11. As in figure 10 starting from the self-trapping regime for $\Lambda = 2 \times 10^3$ s^{-2} and $\eta = 1.6$.

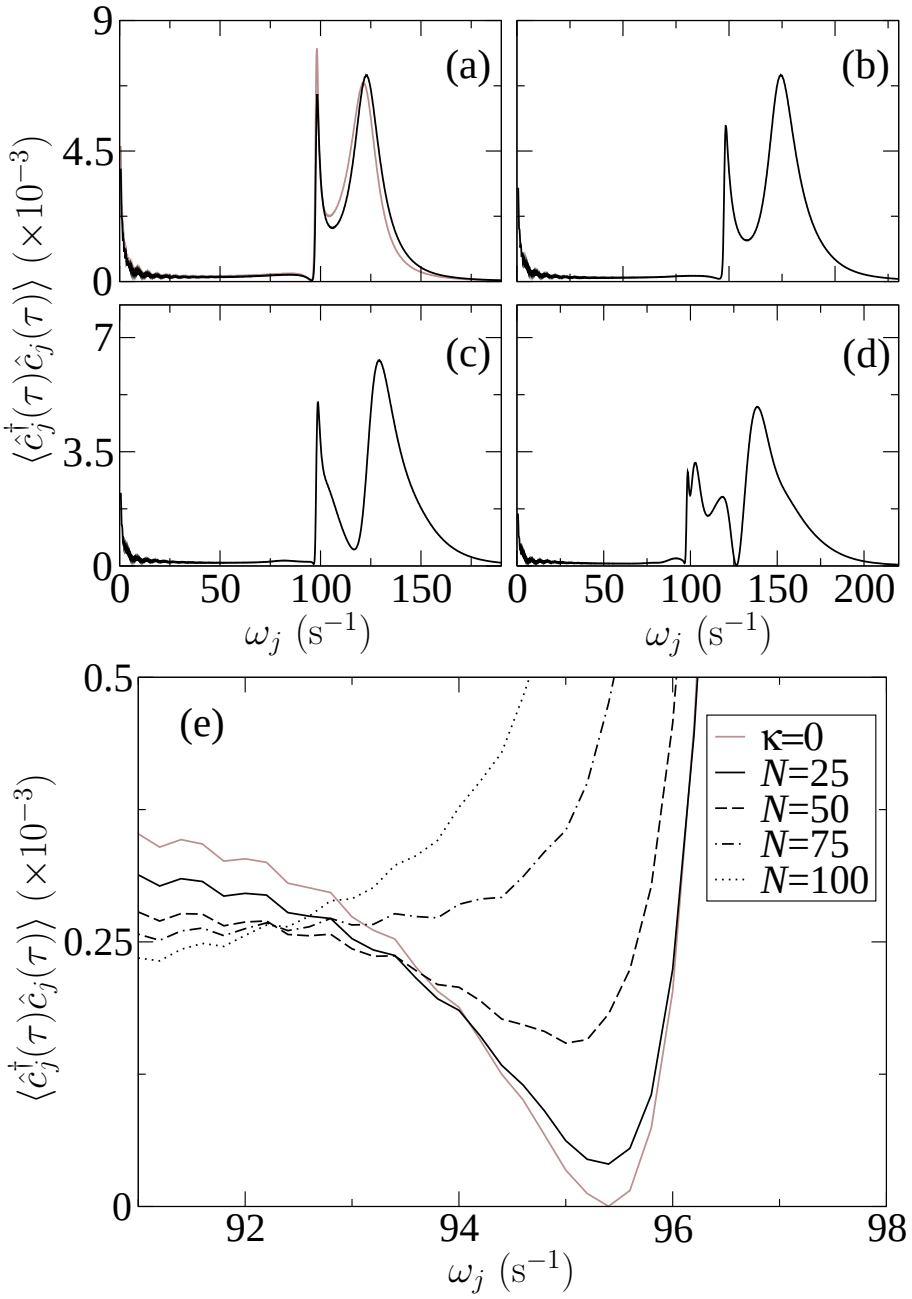

Figure 12. Effects of interatomic interactions on the distribution of outcoupled atoms in the non-Markovian regime. (a-d) Atomic distributions at $\tau = 10$ s for weakly interacting Bose gas with $N = 50$ (a), $N = 100$ (b), $N = 200$ (c) and $N = 300$ (d). Parameters: $\omega_z = 200$ s^{-1}, $\lambda = 0.4$, $\Lambda = 2 \times 10^3$ s^{-2}, $\eta = 1.7$. (e) A closeup of the atomic distribution around the dip for $\Lambda = 10^3$ s^{-2}. The gray curves correspond to an interaction-free Bose gas. Initial conditions: $\tilde{\alpha}(0) = 0.7$, $\tilde{\beta}(0) = 0.3$, $\phi(0) = 0$. Discretization parameters: $M = 1500$, $\omega_{\mathrm{up}} = 300$ s^{-1}.